

Ultra-Fast L2-CL Code Acquisition for a Dual Band GPS Receiver

Binhee Kim, Seung-Hyun Kong[†]

CCS Graduate School for Green Transportation, Korea Advanced Institute of Science and Technology, Daejeon 305-701, Korea

ABSTRACT

GPS L2C signal is a recently added civil signal to L2 frequency and is constructed by time division multiplexing of civil moderate (L2-CM) and civil long (L2-CL) code signals. While the L2-CM code is 20 ms-periodic and modulates satellite navigation message, the L2-CL code is 1.5s-periodic with 767,250 chips long code sequence and carries no data. Therefore, the L2-CL code signal allows receivers to perform a very long coherent integration. However, due to the length of the L2-CL code, the acquisition of the L2-CL code signal may take too long or require too much hardware resources. In this paper, we propose a three-step ultra-fast L2-CL code acquisition (TSCLA) technique for dual band GPS receivers. In the proposed TSCLA technique, a dual band GPS receiver sequentially acquires the coarse/acquisition (C/A) code signal at L1 frequency, the L2-CM code signal, and the L2-CL code signal to minimize mean acquisition time (MAT). The theoretical performance analysis and numerous Monte Carlo simulations show the significant advantage of the proposed TSCLA technique over conventional techniques introduced in the literature.

Keywords: GPS L2C, fast acquisition, civil long code

1. INTRODUCTION

As the new Block IIR-M satellites are deployed according to the GPS modernization plan, L2C signals in L2 frequency are becoming available for receiver positioning. Since 2005, 8 Block IIR-M satellites have been launched and become operational in 2012, and, thanks to the novel code structure of the L2C signal, it is expected that the signal is very useful not only to eliminate ionospheric error but also to improve indoor positioning and tracking performance (Tran & Hegarty 2003, Kaplan & Hegarty 2005, Misra & Enge 2006)

The L2C signal has a 1.023 MHz chip-rate and is constructed by time division multiplexing of two code signals with 511.5 kHz chip-rate; the civil moderate (L2-CM) and civil long (L2-CL) code signals. The 20ms-periodic L2-CM code signal has a code length of 10230 chips and is modulated by navigation message bits at 50bps. On the

other hand, the 1.5 s-periodic L2-CL code signal is a pilot signal and has a long code length of 767,250 chips (Fontana et al. 2001, Dempster 2006, Gernot et al. 2008). Clearly, the L2-CM and L2-CL codes have much longer code period than the C/A code in the L1 frequency (i.e., L1-C/A code), and, therefore, acquiring the L2-CM or L2-CL code signal may take a much longer mean acquisition time (MAT) or may require a lot of hardware resources than the L1-C/A code signal. Since the L2-CM and L2-CL codes have slower chip-rate and much longer code length than the L1-C/A code, the increase of the numbers of code phase hypothesis and Doppler frequency hypotheses results in an even larger search space and huge acquisition complexity for a GPS receiver. There has been a large number of techniques introduced in the literature for the fast acquisition of GPS L1-C/A and L2C signals (Psiaki 2004, Ziedan 2005, Lim et al. 2006, Moghaddam et al. 2006, Qaisar & Dempster 2012, Kong & Kim 2013, Kim & Kong 2014a). For the fast acquisition of the L1-C/A code signal, two-dimensional compressed correlator tests multiple code phase and Doppler frequency hypotheses at once to reduce the MAT by multiple times and is one of the most recent techniques

Received Sep 27, 2015 Revised Nov 23, 2015 Accepted Nov 23, 2015

[†]Corresponding Author

E-mail: skong@kaist.ac.kr

Tel: +82-42-350-1265 Fax: +82-42-350-1250

having small MAT (Kong & Kim 2013, Kim & Kong 2014a). To achieve the fast acquisition of the L2C signal, a number of L2C signal fast acquisition techniques have been introduced in the literature; the Non-Return-to-Zero Twin-Carrier CM code (NRZ TCM) and Non-Return-to-Zero Dual-Channel CM code (NRZ DCM) techniques can reduce MAT for the L2-CM code acquisition when Doppler frequency search space is large or multiple satellite signals are searched (Qaisar & Dempster 2012). However, the improvement with the NRZ TCM and NRZ DCM is limited, since the techniques cannot reduce MAT by more than 2 times than the conventional techniques such as Return-to-Zero CM code (Qaisar & Dempster 2012). There are a number of acquisition techniques using a signal observation from a different frequency band or a different signal; the concept of a fast L2-CM code signal acquisition technique utilizing acquired L1-C/A code signal is introduced briefly (Lim et al. 2006), and, in (Ziedan 2005), a technique is proposed to acquire weak L2-CL code signal from the L2-CM code signal in highly dynamic situations, where a fast acquisition of the L2-CL code signal is not considered. In (Psiaki 2004), the overlap-and-discard technique combined with zero padding is used to compute FFT-based correlation with less computation and to produce partial correlation outputs for the L2-CL acquisition, and, in (Moghaddam et al. 2006), hyper code is introduced and used to achieve a fast L2-CL acquisition at the cost of signal-to-noise-ratio (SNR) degradation.

Despite of the techniques so far, the fast acquisition of L2-CL code signals is still a big challenge. In this paper, we propose an efficient three-step L2-CL acquisition (TSCLA) technique that achieves a very small MAT. In the proposed TSCLA technique, the first step is to acquire the L1-C/A code signal that has much shorter code period and code length than the L2-CM and L2-CL code signals. The second step is to acquire the L2-CM code signal exploiting the knowledge of 1ms epoch found in the first step. In the third step, the L2-CL code signal is acquired utilizing the knowledge of 20ms epoch found in the second step. In the realization of the proposed TSCLA technique, we test two different implementations of the proposed TSCLA technique in employing verification stages; verification process can be employed at the end of each step or used at the end of the third step. We provide theoretical analysis of the detection probability and MAT of the proposed TSCLA technique. It is shown that the proposed TSCLA technique achieves a significant reduction in the acquisition of L2-CL code signal, and we verify the performance with numerous Monte Carlo simulations.

This paper is organized as follows. Section 2 analyzes the

signal structure of the GPS L1 and L2C signals, and Section 3 introduces the proposed TSCLA technique with details. Theoretical performance analysis of the proposed TSCLA technique is shown in Section 4, and the performance of the proposed TSCLA techniques is verified with numerous Monte Carlo simulations in Section 5. The Section 6 provides the conclusion of this paper.

The following notations are used throughout this paper. $(\cdot)_{A'}$, $(\cdot)_{M'}$, and $(\cdot)_{L'}$ denote the parameters for L1-C/A, L2-CM, and L2-CL, respectively, and (\cdot) denotes the estimated parameter.

2. GPS L1/L2 SIGNAL STRUCTURE

Since 2005, 8 Block IIR-M satellites have been launched according to the GPS modernization plan, and the new satellites transmit civil signals such as L1-C/A and L2C whose carrier frequencies are L1 = 1575.42 MHz and L2 = 1227.6 MHz, respectively. The L2C signal has a unique structure; time-division multiplexing of two code signals, of the same chip rate 511.5 kHz, L2-CL (civil long) code signal and L2-CM (civil moderate) code signal that is modulated by 50 Hz binary phase shift keying (BPSK) navigation data $D_M(t)$. Therefore, when we consider the civil code signals transmitted from a new GPS satellite, we can express the signal being transmitted at time t as

$$s(t) = \alpha_1 D_A(t) P_A(t) \cos(2\pi f_{L1} t) + \alpha_2 [D_M(t) P_M(t) H(t) + P_L(t) H(t - T_c)] \times \cos(2\pi f_{L2} t), \quad (1)$$

where

$$H(t) = \frac{1}{2} [\text{sgn}(\sin(2\pi f_{c,2} t)) + 1], \quad (2)$$

α_1 and $\alpha_2 (= \alpha_1 / \sqrt{2})$ represent the signal amplitudes of the L1-C/A and L2C signals, respectively, $D_A(t)$ denotes 50 Hz BPSK navigation data in the L1-C/A code signal, and $P_A(t)$, $P_M(t)$, and $P_L(t)$ are the pseudo-random noise codes for the L1-C/A, L2-CM, and L2-CL code signals, respectively. The chip rate $f_{c,2}$ of the L1-C/A code is 1.023 MHz, while the chip rates of the L2-CM and L2-CL are the same to $f_{c,2} = 511.5$ kHz. Therefore, the chip widths of the L1-C/A, L2-CM, and L2-CL code signals are the same to $T_c = 1/f_{c,1} = 1/(2f_{c,2})$. The periods of the L1-C/A, L2-CM, and L2-CL code signals are $T_{A,p} = 1$ ms, $T_{M,p} = 20$ ms, and $T_{N,p} = 1.5$ s, since the length of the codes are $N_{A,p} = 1023$, $N_{M,p} = 10230$, and $N_{L,p} = 767,250$ chips, respectively. The periods of the code signals are illustrated in Fig. 1, and it should be noted that the chip boundaries of the L1-C/A, L2-CM, and L2-CL

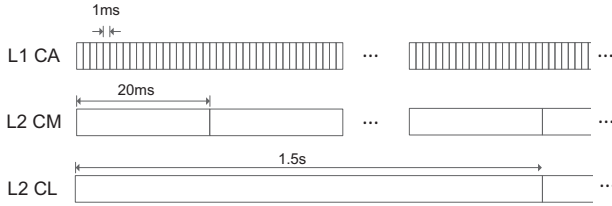


Fig. 1. Code period of L1-C/A, L2-CM, and L2-CL.

codes are perfectly synchronized. Exploiting that the L1-C/A code has shorter period than the L2-CM code and that the L2-CM code has shorter period than the L2-CL code, the acquisition of the L2-CL code signal can be efficiently performed. In the next section, a fast and efficient multi-stage L2-CL acquisition technique is proposed.

3. ULTRA FAST THREE-STEP L2-CL ACQUISITION

Let $r_A(t)$ and $r_C(t)$ denote incoming L1-C/A and L2C code signals transmitted from a Block IIR-M satellite to a dual frequency (i.e., L1 and L2) GPS receiver. In the receiver, $r_A(t)$ and $r_C(t)$ are frequency down-converted to Intermediate Frequency (IF), f_{IF1} and f_{IF2} , respectively, sampled, and summed to yield a sampled IF signal $r[n]$ at $t = nT_s$, where T_s is the sampling interval. In the following analysis, however, we use continuous time expressions that are equivalent to discrete time expressions, for algebraic simplicity. Let $r(t)$ be a continuous time expression equivalent to the $r[n]$, then

$$\begin{aligned}
 r(t) = & \alpha_1 D_A(t - \tau_A) P_A(t - \tau_A) e^{j(2\pi(f_{IF1} + f_{d1})t + \theta_1)} \\
 & + \alpha_2 [D_M(t - \tau_M) P_M(t - \tau_M) H(t - \tau_M) \\
 & + P_L(t - \tau_L) H(t - \tau_L - T_c)] \\
 & \times e^{j(2\pi(f_{IF2} + f_{d2})t + \theta_2)} + w(t),
 \end{aligned} \quad (3)$$

where α_1 denotes the signal amplitude of $r_A(t)$, α_2 denotes the signal amplitude of the received L2-CM and L2-CL code signals, and θ_1 and θ_2 denote the carrier phase of the L1-C/A and L2C signals, respectively. The quantities τ_A , τ_M , and τ_L denote the code phase of the L1-C/A, L2-CM, and L2-CL code signals, respectively, f_{d1} and f_{d2} denote the Doppler frequency of the L1-C/A and L2C code signals, respectively, and $w(t)$ is a complex AWGN with two-sided power spectral density $\frac{N_0}{2}$ over the receiver bandwidth B_r .

3.1 Conventional L2-CL Acquisition

In conventional L2-CL acquisition techniques, a receiver performs an auto-correlation between the IF signal $r(t)$ and a receiver generated signal with a code phase hypothesis

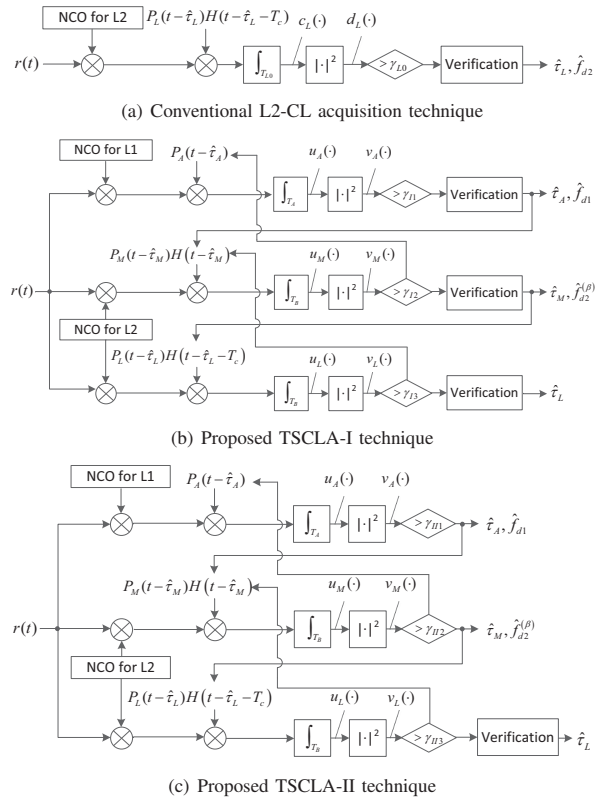


Fig. 2. Schematic diagram of acquisition techniques.

$\tau(t)$ and a Doppler frequency hypothesis to produce an auto-correlation function (ACF) output and its magnitude-squared output as

$$c_L(\hat{\tau}_L, \hat{f}_{d2}) = \int_0^{T_{L0}} r(t) P_L(t - \hat{\tau}_L) H(t - \hat{\tau}_L - T_c) \times e^{-j2\pi(f_{IF2} + \hat{f}_{d2})t} dt \quad (4)$$

$$d_L(\hat{\tau}_L, \hat{f}_{d2}) = |c_{L1}(\hat{\tau}_L, \hat{f}_{d2})|^2 \quad (5)$$

respectively, where T_{L0} denotes the correlation length. The squared ACF output in Eq. (5) is used for the decision to declare signal detection by comparing the maximum value of $d_L(\cdot, \cdot)$ (Eq. (5)) with detection threshold γ_{L0} . Fig. 2a shows the schematic diagram of a conventional L2-CL acquisition technique, where the maximum number of code phase hypotheses to test is $N_{L,C} N_{L,0} = 1,534,500 (\cong 1.5 \times 10^6)$ for a sampling frequency $N_{L,0} = 2$ sample per chip (spc), and the total number of Doppler frequency hypotheses is $(2 \times 10^4 T_{L0} + 1)$ for a frequency search step size $\Delta f_D = \frac{1}{2T_{L0}}$ to search over the $[-5, 5]$ kHz possible Doppler frequency range.

3.2 Proposed Ultra-Fast L2-CL Acquisition

In this subsection, we propose a three-step ultra-fast L2-CL acquisition (TSCLA) technique that employs a sequential acquisition of L1-C/A and L2-CM code signals in

a dual band GPS receiver. The proposed TSCLA technique can have two different realizations depending on the usage of verification stage; verification function can be employed at the end of each of three steps (TSCLA-I), or performed at the end of the third step (TSCLA-II).

In the proposed TSCLA-I technique, the L1-C/A code signal is acquired and verified in the first step, and, in the second step, the L2-CM code signal is searched exploiting the knowledge of $T_{A,p}$ epoch obtained in the first step, and the search result is verified. Finally, in the third step, the L2-CL code signal is searched utilizing the knowledge of $T_{M,p}$ epoch found in the second step, and the search result is verified also. Similar to the proposed TSCLA-I technique, in the proposed TSCLA-II technique, the L1-C/A, L2-CM, and L2-CL code signals are searched in the first, second, and third steps, respectively, and the final search result is verified at the end of the third step.

The first step of the proposed TSCLA-I technique, the receiver performs an auto-correlation between the incoming signal $r(t)$ and the receiver replica of the incoming L1-C/A code signal to obtain an ACF output and its magnitude-squared output as

$$u_A(\hat{t}_A, \hat{f}_{d1}) = \int_0^{T_A} r(t)P_A(t - \hat{t}_A)e^{-j2\pi(f_{IF1} + \hat{f}_{d1})t} dt \quad (6)$$

$$u_A(\hat{t}_A, \hat{f}_{d1}) = |u_A(\hat{t}_A, \hat{f}_{d1})|^2 \quad (7)$$

respectively, where T_A denotes the correlation length. The maximum value of the squared ACF output $u_A(\hat{t}_A, \hat{f}_{d1})$ (Eq. (7)) is compared with a detection threshold γ_{t1} to decide whether the L1-C/A code signal is detected or not. In the first step of the proposed TSCLA-I technique, the total number of code phase hypotheses is $N_{A,p}N_A = 2.046$ for a sampling frequency $N_A = 2$ spc, and the total number of Doppler frequency hypotheses is $(2 \times 10^4 T_A + 1)$ for a frequency search step size $\Delta f_D = \frac{1}{2T_A}$.

If the detection for the L1-C/A code signal is declared and verified successfully, the L2-CM code signal is searched in the second step. Utilizing the knowledge of the $T_{A,p}$ epoch of the L1-C/A code found in the first step, there are only $N_{M,p}/N_{A,p} = 20$ L2-CM code phase hypotheses to test in the second step, since the L1-C/A and L2C code chips are synchronized. However, the search for the Doppler frequency of the L2-CM code signal is not required as it can be directly obtained from the relationship between the Doppler frequencies of the L1-C/A and L2C signals as (Lim et al. 2006)

$$\hat{f}_{d2} = \frac{f_{L2}}{f_{L1}} \hat{f}_{d1} \quad (8)$$

Since the chip rates of the L2-CM and L2-CL codes are

the same and lower than the L1-C/A code, it is useful to have $T_B \geq T_A$, where T_B denotes the same correlation interval used for the second and third steps, and, therefore, T_B/T_A , the number of Doppler frequency hypotheses in the second step corresponding to the single Doppler frequency hypothesis detected in the first step, can be larger than. Using β for the index, the Doppler frequency hypothesis to test in the second step can be expressed as

$$\hat{f}_{d2}^{(\beta)} = \hat{f}_{d2} - \frac{1}{4T_A} + \frac{1}{2T_B} \left(\beta + \frac{1}{2} \right) \quad (9)$$

where $\beta = 0, 1, \dots, T_B/T_A - 1$. Note that the Doppler frequency found in the second step is the unique Doppler frequency to test in the third step.

Using Eq. (8), the receiver performs a correlation between the incoming signal $r(t)$ and the receiver replica signal of the incoming L2-CM code signal to obtain $N_{M,p}/N_{A,p}$ ACF output samples and its magnitude-squared output as

$$u_M(\hat{t}_M, \hat{f}_{d2}^{(\beta)}) = \int_0^{T_B} r(t)P_M(t - \hat{t}_M)H(t - \hat{t}_M) \times e^{-j2\pi(f_{IF2} + \hat{f}_{d2}^{(\beta)})t} dt \quad (10)$$

$$u_M(\hat{t}_M, \hat{f}_{d2}^{(\beta)}) = |u_M(\hat{t}_M, \hat{f}_{d2}^{(\beta)})|^2 \quad (11)$$

respectively, and

$$\hat{t}_M = \hat{t}_A + n_{20}T_{A,p} \quad (12)$$

where $n_{20} \in \{0, 1, 2, \dots, 19\}$. The maximum value of the squared ACF output samples $u_M(\hat{t}_M, \hat{f}_{d2}^{(\beta)})$ (Eq. (11)) is compared with a detection threshold γ_{t2} to decide the detection of the L2-CM code signal.

When the detection and verification of the L2-CM code signal is successful in the second step of the proposed TSCLA-I technique, searching for the L2-CL code signal is performed in the third step. Similar to the second step, making use of the knowledge of $T_{M,p}$ epoch found in the second step, there are only $N_{L,p}/N_{M,p} = 75$ L2-CL code phase hypotheses to test in the third step, and the single Doppler frequency hypothesis $\hat{f}_{d2}^{(\beta)}$ found in the second step is used for all code phase hypothesis testing. The receiver performs a correlation between the incoming signal $r(t)$ and the receiver replica signal of the L2-CL code signal and obtains $N_{L,p}/N_{M,p}$ ACF output samples and its magnitude-squared output as

$$u_L(\hat{t}_M, \hat{f}_{d2}^{(\beta)}) = \int_0^{T_B} r(t)P_L(t - \hat{t}_M)H(t - \hat{t}_M - T_c) e^{-j2\pi(f_{IF2} + \hat{f}_{d2}^{(\beta)})t} dt \quad (13)$$

$$u_L(\hat{t}_M, \hat{f}_{d2}^{(\beta)}) = |u_L(\hat{t}_M, \hat{f}_{d2}^{(\beta)})|^2 \quad (14)$$

respectively, where T_B denotes the correlation interval, and

$$\hat{\tau}_L = \hat{\tau}_M + n_{75} T_{M,P}, \quad (15)$$

where $n_{75} \in \{0, 1, 2, \dots, 19\}$. The maximum value of the squared ACF output samples $u_L(\hat{\tau}_M, \hat{f}_{d2}^{(\beta)})$ (Eq. (14)) is compared with a detection threshold γ_{I3} to decide if the L2-CL code signal is detected. Finally, if the L2-CL code signal detection is declared in the third step, the detected code phase $\hat{\tau}_L$ and the Doppler frequency $\hat{f}_{d2}^{(\beta)}$ are further tested p times for a verification.

Similar to the proposed TSCLA-I technique, the proposed TSCLA-II technique searches L1-C/A, L2-CM, and L2-CL code signals in the first, second, and third steps with detection thresholds γ_{II1} , γ_{II2} , and γ_{II3} , respectively. The algorithm of the proposed TSCLA-II technique is similar to that of the proposed TSCLA-I technique, except that the verification stage is only at the end of the third step. Figs. 2b and c show the schematic diagram of the proposed TSCLA-I and TSCLA-II techniques, respectively.

4. PERFORMANCE ANALYSIS

In this section, we derive mathematical expressions to analyze the acquisition performance of the proposed TSCLA technique in terms of detection probabilities and MAT.

The noise variances of the first, second, and third steps of the proposed TSCLA-I technique are

$$V_1 = T_A N_A N_0 / T_C \quad (16)$$

$$V_2 = T_B N_B N_0 / (2T_C) \quad (17)$$

$$V_3 = T_B N_B N_0 / (2T_C), \quad (18)$$

respectively, where N_B denotes a sampling frequency for the L2C signal. And the noise variances of the first, second, and third steps of the proposed TSCLA-II technique are the same to those of the proposed TSCLA-I technique. The expected peak magnitudes of the ACF outputs at the three steps of the proposed TSCLA-I and TSCLA-II techniques, $v_A(\cdot, \cdot)$ (Eq. (6)), $v_B(\cdot, \cdot)$ (Eq. (10)), and $v_L(\cdot, \cdot)$ (Eq. (13)), are found as

$$S_1 = E[|R_A(\hat{\tau}_A, \hat{f}_{d1})|] = \frac{1}{T_A} E \left[\int_{\tau_A}^{\tau_A + T_A} P_A(u - \tau_A) \times e^{j(2\pi\delta f_{d1} u + \theta_1)} du \right] \\ = \frac{\sin(\pi\delta f_{d1} T_A)}{\pi\delta f_{d1} T_A} \cdot \frac{\sin(\pi\delta f_{d1} (T_C - |\delta\tau_A|))}{\pi\delta f_{d1} T_C} \quad (19)$$

$$S_2 = E[|R_M(\hat{\tau}_M, \hat{f}_{d2}^{(\beta)})|] = \frac{1}{T_B} E \left[\int_{\tau_M}^{\tau_M + T_B} P_M(u - \tau_M) P_M(u - \hat{\tau}_M) \times H(u - \hat{\tau}_M) e^{j(2\pi\delta f_{d2}^{(\beta)} u + \theta_2)} du \right] \\ = \frac{\sin(\pi\delta f_{d2}^{(\beta)} T_B)}{\pi\delta f_{d2}^{(\beta)} T_B} \cdot \frac{\sin(\pi\delta f_{d2}^{(\beta)} (T_C - |\delta\tau_M|))}{\pi\delta f_{d2}^{(\beta)} T_B} \quad (20)$$

$$S_3 = E[|R_L(\hat{\tau}_L, \hat{f}_{d2}^{(\beta)})|] = \frac{1}{T_B} E \left[\int_{\tau_L}^{\tau_L + T_B} P_L(u - \tau_L) P_L(u - \hat{\tau}_L) \times H(u - \hat{\tau}_L - T_C) e^{j(2\pi\delta f_{d2}^{(\beta)} u + \theta_2)} du \right] \\ = \frac{\sin(\pi\delta f_{d2}^{(\beta)} T_B)}{\pi\delta f_{d2}^{(\beta)} T_B} \cdot \frac{\sin(\pi\delta f_{d2}^{(\beta)} (T_C - |\delta\tau_L|))}{\pi\delta f_{d2}^{(\beta)} T_B} \quad (21)$$

respectively, where t_0 is the time when the correlation function starts, and

$$|\delta\tau_A| = |\tau_A - \hat{\tau}_A| \leq T_C / (2N_A) \quad (22)$$

$$|\delta\tau_M| = |\tau_M - \hat{\tau}_M| \leq T_C / (2N_B) \quad (23)$$

$$|\delta\tau_L| = |\tau_L - \hat{\tau}_L| \leq T_C / (2N_B) \quad (24)$$

$$|\delta f_{d1}| = |f_{d1} - \hat{f}_{d1}| \leq 1 / (2T_A) \quad (25)$$

$$|\delta f_{d2}^{(\beta)}| = |f_{d2} - \hat{f}_{d2}^{(\beta)}| \leq 1 / (2T_B) \quad (26)$$

In the following expressions, V_j , S_j , and γ_{ij} represent the noise variance, expected peak magnitude of ACF output, and detection threshold of the j th step of the proposed TSCLA- i technique, respectively, where j represents index for the three steps such that $j=1, 2, \text{ or } 3$, and i denotes the index of the proposed technique such that $i=I$ or II . Note that $j=0$ denotes the conventional L2-CL acquisition technique whose noise variance and the expected peak magnitude are $V_0 = V_3$ and $S_0 = S_3$, respectively.

When the acquisition is successful, the detection variables $v_A(\cdot, \cdot)$ (Eq. (7)), $v_B(\cdot, \cdot)$ (Eq. (11)) and $v_L(\cdot, \cdot)$ (Eq. (14)) are represented by Y that has a noncentral χ^2 distribution with two degrees of freedom (Viterbi 1995)

$$P_{1,j}(Y) = \frac{1}{V_j} \exp\left(\frac{-(Y + S_j^2)}{V_j}\right) I_0\left(\frac{2S_j \sqrt{Y}}{V_j}\right) \quad (27)$$

where $I_0(\cdot)$ is the zeroth-order modified Bessel function of the first kind. When the acquisition is not successful, i.e., the current hypothesis is not close enough to the true code phase and Doppler frequency, the detection variables $v_A(\cdot, \cdot)$, $v_B(\cdot, \cdot)$, and $v_L(\cdot, \cdot)$ are denoted by X that has a central χ^2 distribution with two degrees of freedom (Viterbi 1995)

$$P_{0,j}(X) = \frac{1}{v_j} \exp\left(\frac{-x}{v_j}\right) \quad (28)$$

Using $P_{1,j}(Y)$ (Eq. (27)) and $P_{0,j}(X)$ (Eq. (28)), the detection, misdetection, and false alarm probabilities can be found as (Viterbi 1995)

$$P_{D,j} = \int_{\gamma_{ij}}^{\infty} P_{1,j}(Y) dY = \int_{\gamma_{ij}/V_j}^{\infty} e^{-x + \frac{S_j^2}{V_j}} I_0\left(2\sqrt{\frac{S_j^2 x}{V_j}}\right) dx \\ = Q\left(S_j \sqrt{\frac{2}{V_j}}, \sqrt{\frac{2\gamma_{ij}}{V_j}}\right) \quad (29)$$

$$P_{M,j} = 1 - P_{D,j} \quad (30)$$

$$P_{F,j} = \int_{\gamma_{ij}}^{\infty} P_{0,j}(X) dX = \exp\left(-\frac{\gamma_{ij}}{V_j}\right) \quad (31)$$

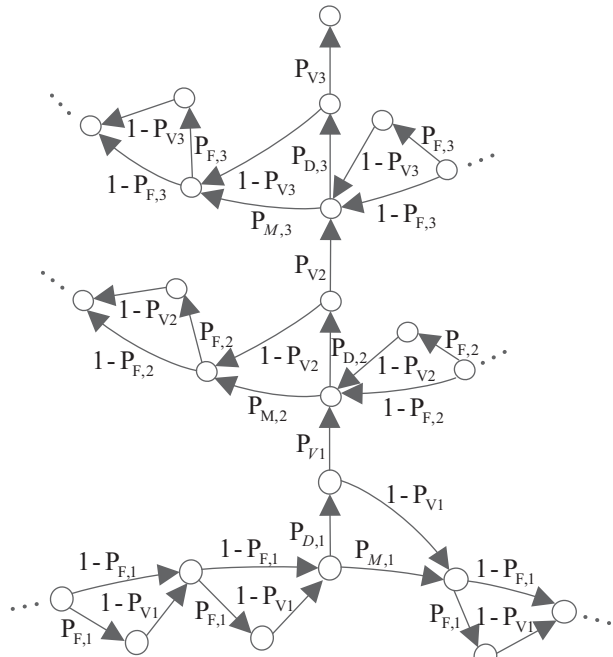


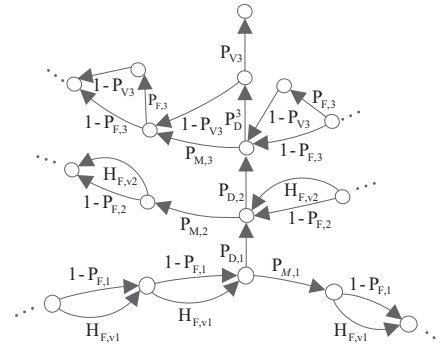
Fig. 3. Circular search diagram of proposed TSCLA technique-I.

where $Q(a,b)$ is the Marcum's Q-function (Marcum 1950).

Figs. 3 and 4 show the circular search state diagrams of the proposed TSCLA-I and TSCLA-II techniques, respectively. In the proposed TSCLA-I and TSCLA-II techniques, when the current hypothesis of the j th step is correct for $j=1, 2, 3$, the hypothesis testing may have a successful signal detection with $P_{D,j}$ or miss the signal detection with probability $P_{M,j}$. On the other hand, when the current hypothesis of the j th step is incorrect, it may conclude the absence of signal with a probability $1-P_{F,j}$ or may result in a false alarm with probability $P_{F,j}$. When signal detection is declared in the j th step, verification process that has a detection probability P_{V_j} tests the detected hypothesis for p times. Notice that $P_{.j}$ represents a probability in the j th step for $j \leq 3$. When the signal detection is verified in the j th step and $j < 3$, the proposed TSCLA-I technique proceeds to the $(j+1)$ th step. In the proposed TSCLA-II technique, however, when signal detection is declared in the j th step for $j < 3$, the proposed TSCLA-II technique proceeds to the $(j+1)$ th step without a verification process. When the signal detection is declared in the third step, verification process that has a detection probability P_{V_3} tests the detected hypothesis p times.

From Fig. 3, the overall transfer function for the proposed TSCLA technique-I can be found as

$$H_I(T) = \frac{H_{D,I}(T) [1 - H_{0,I}^{N_1 F_n}(T)]}{N_1 F_n [1 - H_{0,I}(T)] [1 - H_{M,I}(T) H_{0,I}^{N_1 F_n - 1}(T)]} \quad (32)$$



(a) Simplified state diagram of proposed TSCLA technique-II

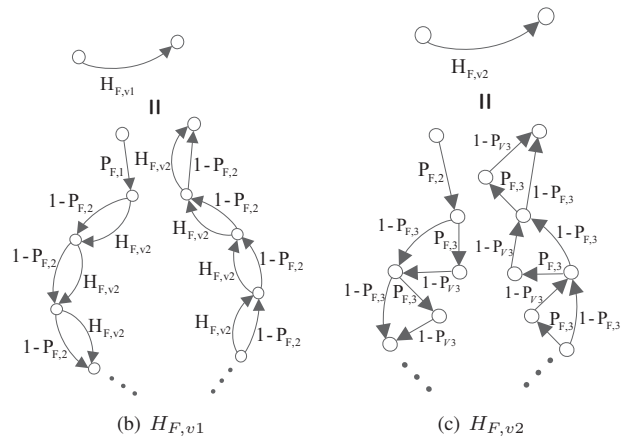


Fig. 4. Circular search diagram of proposed TSCLA technique-II.

where $N_1 (= N_{A,p} N_A)$ denotes the number of code phase hypotheses, $F_n (= 2 \times 10^4 T_A + 1)$ denotes the number of Doppler frequency hypotheses in the first step,

$$H_{D,I}(T) = P_{D,1} T^{p+1} H_{I,2}(T) \quad (33)$$

$$H_{M,I}(T) = P_{M,1} T \quad (34)$$

$$H_{0,I}(T) = (1 - P_{F,1}) T + P_{F,1} T^{p+1} \quad (35)$$

and pT denotes the penalty time taken for a verification process. The algebraic expression for in Eq. (33) is

$$H_{I,2}(T) = \frac{H_{D,I,2}(T) [1 - H_{0,I,2}^{N_2}(T)]}{N_2 [1 - H_{0,I,2}(T)] [1 - H_{M,I,2}(T) H_{0,I,2}^{N_2 - 1}(T)]} \quad (36)$$

where the number of hypotheses in the second step is

$$N_2 = \frac{N_{M,p} T_B}{N_{A,p} T_A} \quad (37)$$

$\beta_1 = T_B / T_A$ denotes the ratio between the integration time at the second and third step (T_B) and the first step (T_A), and

$$H_{D,I,2}(T) = P_{D,2} T^{(p+1)\beta_1} H_{I,3}(T) \quad (38)$$

$$H_{M,I2}(T) = P_{M,2}T^{\beta}, \quad (39)$$

$$H_{0,I2}(T) = (1-P_{F,2})T^{\beta} + P_{F,2}T^{(p+1)\beta}, \quad (40)$$

The algebraic expression for $H_{I,3}(T)$ in Eq. (38) is

$$H_{I,3}(T) = \frac{H_{D,I3}(T)[1-H_{0,I3}^{N_3}(T)]}{N_3[1-H_{0,I3}(T)][1-H_{M,I3}(T)H_{0,I3}^{N_3-1}(T)]} \quad (41)$$

where $N_3(=N_{L,p}/N_{M,p})$ denotes the number of code phase hypotheses in the third step, and

$$H_{D,I3}(T) = P_{D,3}T^{(p+1)\beta}, \quad (42)$$

$$H_{M,I3}(T) = P_{M,3}T^{\beta}, \quad (43)$$

$$H_{0,I3}(T) = (1-P_{F,3})T^{\beta} + P_{F,3}T^{(p+1)\beta}, \quad (44)$$

From Fig. 4, the overall transfer function for the proposed TSCLA-II technique can be found as

$$H_{II}(T) = \frac{H_{D,II}(T)[1-H_{0,II}^{N_1F_n}(T)]/(N_1F_n)}{[1-H_{0,II}(T)][1-H_{M,II}(T)H_{0,II}^{N_1F_n-1}(T)]} \quad (45)$$

where

$$H_{D,II}(T) = P_{D,1}TH_{I,2}(T) \quad (46)$$

$$H_{M,II}(T) = P_{M,1}T \quad (47)$$

$$H_{0,II}(T) = (1-P_{F,1})T + H_{F,II1}(T) \quad (48)$$

and

$$H_{F,II1}(T) = P_{F,1}T((1-P_{F,2})T^{\beta} + H_{F,II2}(T))^{N_2} \quad (49)$$

$$H_{F,II2}(T) = P_{F,2}T^{\beta}((1-P_{F,3})T^{\beta} + (P_{F,3})T^{(p+1)\beta})^{N_3}. \quad (50)$$

The algebraic expression for $H_{II,2}$ in Eq. (46) is

$$H_{II,2}(T) = \frac{H_{D,II2}(T)[1-H_{0,II2}^{N_2}(T)]/N_2}{[1-H_{0,II2}(T)][1-H_{M,II2}(T)H_{0,II2}^{N_2-1}(T)]} \quad (51)$$

where

$$H_{D,II2}(T) = P_{D,2}T^{\beta}H_{I,3}(T) \quad (52)$$

$$H_{M,II2}(T) = P_{M,2}T^{\beta} \quad (53)$$

$$H_{0,II2}(T) = (1-P_{F,2})T^{\beta} + H_{F,II2}(T) \quad (54)$$

And the expression for $H_{I,3}(T)$ in Eq. (52) is found as

$$H_{I,3}(T) = \frac{H_{D,II3}(T)[1-H_{0,II3}^{N_3}(T)]/N_3}{[1-H_{0,II3}(T)][1-H_{M,II3}(T)H_{0,II3}^{N_3-1}(T)]} \quad (55)$$

where

$$H_{D,II3}(T) = P_{D,3}T^{(p+1)\beta} \quad (56)$$

$$H_{M,II3}(T) = P_{M,3}T^{\beta} \quad (57)$$

$$H_{0,II3}(T) = (1-P_{F,3})T^{\beta} + P_{F,3}T^{(p+1)\beta} \quad (58)$$

For a comparison, the overall transfer function for the conventional L2-CL acquisition technique (Abu-Rgheff 2007, Kim & Kong 2014b) is

$$H_c(T) = \frac{H_{D,c}(T)[1-H_{0,c}^{N_c}(T)]}{N_c[1-H_{0,c}(T)][1-H_{M,c}(T)H_{0,c}^{N_c-1}(T)]} \quad (59)$$

where $N(=N_{L,p}N_{L,0})$ denotes the number of code phase hypotheses for the conventional L2-CL acquisition technique, $F_c(=2 \times 10^{-4}T_{L,0}+1)$ denotes the number of Doppler frequency hypotheses for the conventional L2-CL acquisition technique, and the branch transfer function for the correct hypothesis detection, correct hypothesis missed, and incorrect hypothesis are

$$H_{D,c}(T) = P_{D,0}T^{p+1} \quad (60)$$

$$H_{M,c}(T) = P_{M,0}T \quad (61)$$

$$H_{0,c}(T) = (1-P_{F,0})T + P_{F,0}T^{p+1} \quad (62)$$

respectively.

Using Eq. (32), the MAT of the proposed TSCLA-I technique is derived as

$$\begin{aligned} \mu_t &= \left. \frac{dH_I(T)}{dT} \right|_{T=1} \times T_A \\ &= \left[\frac{P_{M,1}}{1-P_{M,1}}(1+(N_1F_n-1)(1+pP_{F,1})) \right. \\ &\quad + \frac{\beta_1 P_{M,2}}{1-P_{M,2}}(1+(N_2-1)(1+pP_{F,2})) \\ &\quad + \frac{\beta_1 P_{M,3}}{1-P_{M,3}}(1+(N_3-1)(1+pP_{F,3})) \\ &\quad + \frac{N_1F_n-1}{2}(1+pP_{F,1}) + \frac{\beta_1(N_2-1)}{2}(1+pP_{F,2}) \\ &\quad \left. + \frac{\beta_1(N_3-1)}{2}(1+pP_{F,3}) + (2\beta_1+1)(p+1) \right] T_A \quad (63) \end{aligned}$$

which, for high SNR, can be simplified to

$$\mu_t|_{\text{SNR} \uparrow} = \left[(2\beta_1+1)p + \frac{N_1F_n + \beta_1(N_2+N_3+2)}{2} \right] T_A \quad (64)$$

Note that the expression for $\mu_t|_{\text{SNR} \uparrow}$ (Eq. (64)) can be expected, since there are three verification process that requires $3p$ correlations, and the expected number of hypothesis during the three search steps is $(N_1F_n+N_2+N_3+3)/2$ in the proposed TSCLA-I technique. Similarly, the MAT of

the proposed TSCLA-II technique is found from Eq. (45) as

$$\begin{aligned} \mu_{II} &= \left. \frac{dH_{II}(T)}{dT} \right|_{T=1} \times T_A \\ &= \left[\frac{P_{M,1}}{1-P_{M,1}} (1+(N_1 F_n - 1)) \right. \\ &\quad \times (1 + \beta_i P_{F,1} N_2 (1 + P_{F,2} N_3 (1 + p P_{F,3}))) \\ &\quad + \frac{\beta_i P_{M,2}}{1-P_{M,2}} (1+(N_2 - 1)(1 + P_{F,2} N_3 (1 + p P_{F,3}))) \\ &\quad + \frac{\beta_i P_{M,3}}{1-P_{M,3}} (1+(N_3 - 1)(1 + p P_{F,3})) \\ &\quad + \frac{N_1 F_n - 1}{2} (1 + \beta_i P_{F,1} N_2 (1 + P_{F,2} N_3 (1 + p P_{F,1}))) \\ &\quad + \frac{\beta_i (N_2 - 1)}{2} (1 + P_{F,2} N_3 (1 + p P_{F,2})) \\ &\quad \left. + \frac{\beta_i (N_3 - 1)}{2} (1 + p P_{F,3}) + (p + 2)\beta_i + 1 \right] T_A \end{aligned} \tag{65}$$

and μ_{II} for high SNR becomes

$$\mu_{II}|_{SNR \uparrow} = \left[p\beta_i + \frac{N_1 F_n + \beta_i (N_2 + N_3 + 2) + 1}{2} \right] T_A \tag{66}$$

Note that the $\mu_{II}|_{SNR \uparrow}$ is smaller than $\mu_I|_{SNR \uparrow}$ by $2p$ as expected. However, since $N_1 F_n / 2 \gg 3p$, it is expected that $\mu_I|_{SNR \uparrow} \approx \mu_{II}|_{SNR \uparrow}$. On the other hand, the MAT of the conventional L2-CL acquisition technique is

$$\begin{aligned} \mu_c &= \left. \frac{dH_c(T)}{dT} \right|_{T=1} \times T_{L0} \\ &= \left[p + \frac{1 + p P_{F,0}}{P_{D,0}} + \left(\frac{1}{P_{D,0}} - \frac{1}{2} \right) \right. \\ &\quad \left. \times (1 + p P_{F,0})(N F_c - 1) \right] T_{L0} \end{aligned} \tag{67}$$

so that μ_c for high SNR, becomes

$$\mu_c|_{SNR \uparrow} = \left[p + \frac{N F_c + 1}{2} \right] T_{L0} \tag{68}$$

Note that since $N_1 F_n / 2 \gg 3p$, $\mu_c|_{SNR \uparrow}$ is about $(N F_c T_{L0}) / (N_1 F_n T_A) \approx 3000$ times larger than $\mu_I|_{SNR \uparrow}$ and $\mu_{II}|_{SNR \uparrow}$ for $T_{L0} = 2$ ms and $T_A = 1$ ms.

5. NUMERICAL RESULTS

In this section, we provide the results of 10^4 Monte Carlo simulations to compare the proposed TSCLA techniques with the conventional L2-CL acquisition technique. In the simulations, $T_A = 1$ ms, $T_B = T_{L0} = 2$ ms, and $N_A = N_B = N_{L,0} = 2$ spc are used for a common choice used in GPS receivers, and

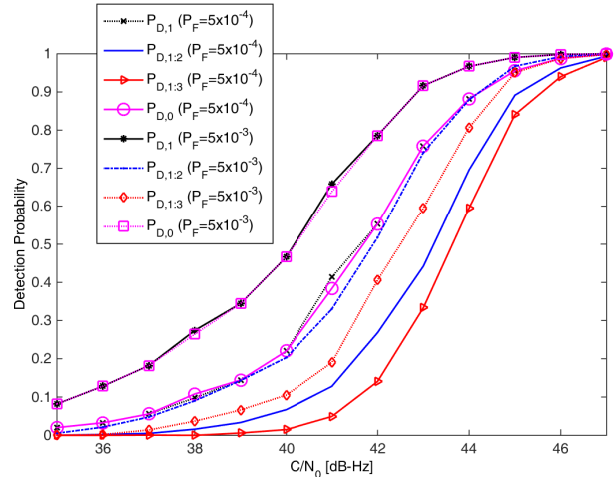


Fig. 5. Detection probability.

the Doppler frequency search step size Δf_D used for the first step of the proposed TSCLA technique is $1/(2T_A)$, and that used for the second and third steps of the proposed TSCLA technique and that used for the conventional technique are the same to $1/(2T_B)$. In addition, the receiver pre-correlation bandwidth (van Diggelen 2009) is assumed to be $2f_{c,1} = 2.046$ MHz.

Fig. 5 shows overall detection probabilities upto the three steps of the proposed TSCLA technique and the detection probability of the conventional technique for a constant false alarm rate (CFAR) $P_F = 5 \times 10^{-4}$ and $P_F = 5 \times 10^{-3}$, where the overall detection probability upto the j th step of the proposed TSCLA technique is obtained by

$$P_{D,1:j} = \prod_{k=1}^j P_{D,k} \tag{69}$$

As expected, it is found that $P_{D,0} = P_{D,1}$ for all CFAR, and that the overall detection probabilities upto the second and third steps, i.e., $P_{D,1:2}$ and $P_{D,1:3}$, are much lower than the detection probability of the conventional technique for all CFAR values tested. However, we can see that $P_{D,1:2}$ and $P_{D,1:3}$ for a higher CFAR is higher than those for a lower CFAR. Notice that $P_{D,1:j}$'s ($j = 1, 2, 3$) for the proposed TSCLA-I technique are the same to those for the proposed TSCLA-II technique, since $P_V \approx 1$ is assumed.

Fig. 6 shows that the MAT of the proposed TSCLA-I and TSCLA-II techniques can be significantly smaller than the conventional technique for $C/N_0 > 35$ dB-Hz. As C/N_0 falls below 46 dB-Hz as observed from Fig. 5, the difference between $P_{D,0}$ and $P_{D,1:3}$ increases and the MAT difference between the TSCLA and the conventional techniques becomes smaller; when the incoming GPS signal is strong, the proposed TSCLA technique achieves about 2800 times smaller MAT than the conventional technique for

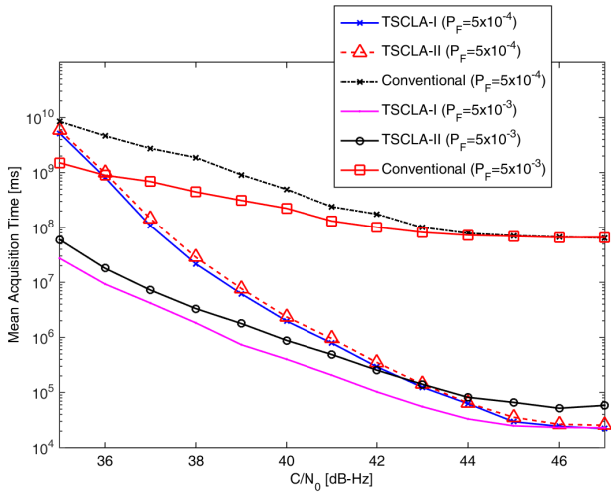


Fig. 6. Mean acquisition time.

both CFAR values tested. However, the proposed TSCLA techniques achieve only at least 250 and 25 times smaller MAT than the conventional technique when is about 40 dB-Hz and 35 dB-Hz, respectively, for CFAR $P_F=5\times 10^{-3}$, and achieve about 160 and 1.5 times smaller MAT than the conventional technique when C/N_0 is around 40 dB-Hz and 35 dB-Hz, respectively, for smaller CFAR $P_F=5\times 10^{-4}$. This shows that the advantage of the proposed TSCLA technique over the conventional technique decreases as C/N_0 and P_F decrease below 45 dB-Hz and about $P_F=5\times 10^{-3}$, respectively. For $P_F=5\times 10^{-3}$, the proposed TSCLA-I technique has a slightly lower MAT than the proposed TSCLA-II technique, while the proposed TSCLA-I technique has almost same MAT with the proposed TSCLA-II for $P_F=5\times 10^{-4}$. This is because the proposed TSCLA-I technique has lower penalty time for the false alarm than the proposed TSCLA-II technique.

Fig. 7 shows that t-e MAT of the proposed TSCLA-I and TSCLA-II techniques with respect to a range of CFAR from $P_F=10^{-5}$ to $P_F=5\times 10^{-3}$, when an incoming GPS signal has $C/N_0=47$ dB-Hz. As shown, the performance of the proposed TSCLA-I technique is slightly better than the TSCLA-II for CFAR lower than $P_F=10^{-4}$, however, the performance of the proposed TSCLA-II technique becomes noticeably poorer than the proposed TSCLA-I technique for CFAR higher than $P_F=10^{-4}$, which shows that the proposed TSCLA-I technique is robust to noisy detection (i.e., high false alarm rate). Note that we use $p=10$ in all simulations, and when p is sufficiently larger than 10, the performance difference between the proposed TSCLA-I and TSCLA-II techniques can be negligible or it maybe possible to have an opposite performance pattern to what is shown in Fig. 7 for CFAR lower than $P_F=10^{-4}$.

To summarize, in a good signal condition, the proposed TSCLA-I technique has much smaller MAT than the

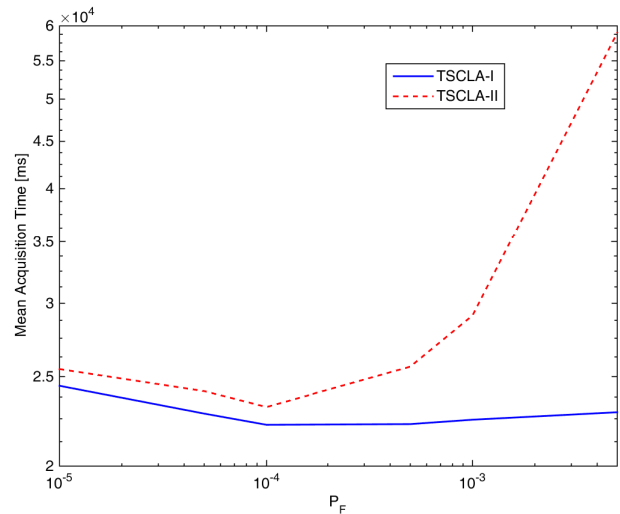


Fig. 7. Mean acquisition time with respect to CFAR.

conventional technique that searches all the hypotheses of L2-CL. This is because the number of hypotheses to be searched is much smaller since the proposed TSCLA-I technique searches a hypothesis in the order of L1-CA, L2-CM, and L2-CL and because there is a high possibility of searching a correct hypothesis without verification when the signal condition is good.

6. CONCLUSIONS

A three-step L2-CL code signal acquisition technique has been proposed for a dual band GPS receiver performing a serial search. In the first step of the proposed technique, the GPS receiver acquires the C/A code signal at L1 frequency, and, in the second and third steps of the proposed technique, the receiver acquires the CM and CL code signals at L2 frequency sequentially. The detection probability and MAT of the proposed technique have been analyzed theoretically and verified with numerous Monte Carlo simulations. It has been found that the proposed TSCLA-I technique can achieve a much faster L2-CL code signal acquisition than the conventional technique and that the MAT improvement can be significant. Since the L2-CL code signal is a pilot signal useful to improve receiver sensitivity easily, the proposed technique is beneficial for dual band GPS receivers to acquire L2-CL code signals.

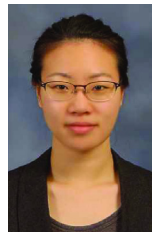
ACKNOWLEDGMENTS

This research (2013R1A2A2A01067863) was supported by Mid-career Researcher Program through NRF grant funded

by the Korean government (MEST).

REFERENCES

- Abu-Rgheff, M. A. 2007, Introduction to CDMA Wireless Communications (CA: Academic Press)
- Dempster, A. G. 2006, Correlators for L2C: Some considerations, *Inside GNSS*, 1(7), 32-37, Oct. 2006, <http://www.insidegnss.com/auto/1006%20Correlators.pdf>
- Fontana, R. D., Cheung, W., Novak, P. M., & Stansell, Jr. T. A. 2001, The new L2 civil signal, in 2001 ION GNSS, Salt Lake City, UT, 2001
- Gernot, C., O'Keefe, K., & Lachapelle, G. 2008, Comparison of L1 C/A-L2C combined acquisition techniques, in 2008 ENC, Toulouse, France, 2008
- Kaplan, E. D. & Hegarty, C. J. 2005, Understanding GPS: Principles and Applications, 2nd ed. (MA: Artech House)
- Kim, B. & Kong, S. H. 2014a, Design of FFT-based TDCC for GNSS Acquisition, *IEEE Trans. on Wirel. Commun.*, 13, 2798-2808, <http://ieeexplore.ieee.org/stamp/stamp.jsp?tp=&number=6786057>
- Kim, B. & Kong, S.-H. 2014b, Determination of Detection Parameters on TDCC Performancem, *IEEE Trans. Wirel. Commun.*, 13, 2422-2431, <http://ieeexplore.ieee.org/stamp/stamp.jsp?tp=&number=6733255>
- Kong, S. H. & Kim, B. 2013, Two-Dimensional Compressed Correlator for Fast PN Code Acquisition, *IEEE Trans. on Wirel. Commun.*, 12, 5859-5867, <http://dx.doi.org/10.1109/TWC.2013.092313.130407>
- Lim, D. W., Moon, S. W., Park, C., & Lee, S. J. 2006, L1/L2CS GPS receiver implementation with fast acquisition scheme, in 2006 IEEE/ION PLANS, San Diego, CA, Apr. 2006, pp.840-844, <http://www.ion.org/publications/abstract.cfm?articleID=6722>
- Marcum, J. I. 1950, A Table of Q-functions, Rand Corp. Report, RM-339, Jan. 1950
- Misra, P. & Enge, P. 2006, Global Positioning System: Signals, Measurements, and Performance, 2nd ed. (MA: Ganga-Jamuna Press)
- Moghaddam, A. R. A., Watson, R., Lachapelle, G., & Nielsen, J. 2006, Exploiting the orthogonality of L2C code delays for a fast acquisition, in 2006 ION GNSS, Fort Worth, TX, Sep. 2006
- Psiaki, M. L. 2004, FFT-based acquisition of GPS L2 Civilian CM and CL signals, in 2004 ION GNSS, Long Beach, CA, Sep. 2004
- Qaisar, S. U. & Dempster, A. G. 2012, Assessment of the GPS L2C code structure for efficient signal acquisition, *IEEE Trans. Aero. Electron. Sys.*, 48, 1889-1902, <http://dx.doi.org/10.1109/TAES.2012.6237568>
- Tran, M. & Hegarty, C. 2003, Performance evaluations of the new GPS L5 and L2 civil signals, in 2003 ION NTM, Anaheim, CA, USA, 2003
- van Diggelen, F. 2009, A-GPS: Assisted GPS, GNSS, and SBAS (MA: Artech House), pp.31-60
- Viterbi, A. J. 1995, CDMA: Principles of Spread Spectrum Communication (CA: Addison-Wesley Publishing Company)
- Ziedan, N. I. 2005, Acquisition and fine acquisition of weak GPS L2C and L5 signals under high dynamic conditions for limited-resource applications, in 2005 ION GNSS, Long Beach, CA, Sep. 2005



Binhee Kim received B.S. and M.S. degrees in electrical engineering from Korea Advanced Institute of Science and Technology (KAIST), Daejeon, Korea, in 2008 and 2010, respectively. She is a researcher in the CCS Graduate School for Green Transportation at KAIST, where she received a Ph.D. degree in 2015. Her research

interests include radar signal processing, GNSS signal processing, and detection and estimation for navigation systems.



Seung-Hyun Kong received a B.S.E.E. from Sogang University, Korea, in 1992, an M.S.E.E. from Polytechnic University, New York, in 1994, and a Ph.D. degree in aeronautics and astronautics from Stanford University, CA, in 2006. From 1997 to 2004, he was with Samsung Electronics Inc. and Nxpilot Inc.,

both in Korea, where his research focus was on 2G CDMA and 3G UMTS PHY and mobile positioning technologies. In 2006, he was involved with hybrid positioning technology development using wireless location signature and Assisted GNSS at Polaris Wireless, Inc. and from 2007 to 2009, he was a research staff at Qualcomm Research Center, San Diego, CA, where his R&D focused on indoor location technologies and advanced GNSS technologies. Since 2010, he has been an Assistant Professor at the Department of Aerospace Engineering in the Korea Advanced Institute of Science and Technology (KAIST). His research interests include super-resolution signal processing, detection and estimation for navigation systems, and assisted GNSS in wireless communication systems.